JAERI-M--94-001

JP9406027

JAERI-M
94-001

DEVELOPMENT OF OXIDATION RESISTANT SiC/C COMPOSITIONALLY GRADIENT MATERIALS

January 1994

Kimio FUJII, Junichi NAKANO
and Masami SHINDO

日 本 原 子 力 研 究 所
Japan Atomic Energy Research Institute

JAERI-Mレポートは、日本原子力研究所が不定期に公刊している研究報告書です。

入手の問合わせは、日本原子力研究所技術情報部情報資料課（〒319-11 茨城県那珂郡東海村）あて、お申しこしください。なお、このほかに財団法人原子力弘済会資料センター（〒319-11 茨城県那珂郡東海村日本原子力研究所内）で複写による実費頒布をおこなっております。

JAERI-M reports are issued irregularly.

Inquiries about availability of the reports should be addressed to Information Division Department of Technical Information, Japan Atomic Energy Research Institute, Tokaimura, Naka-gun, Ibaraki-ken 319-11, Japan.

© Japan Atomic Energy Research Institute, 1994

編集兼発行　日本原子力研究所
印　　　刷　ニッセイエブロ株式会社

Development of Oxidation Resistant SiC/C Compositionally Gradient Materials

Kimio FUJII, Junichi NAKANO and Masami SHINDO

Department of Materials Science and Engineering
Tokai Research Establishment
Japan Atomic Energy Research Institute
Tokai-mura, Naka-gun, Ibaraki-ken

(Received January 5, 1994)

For the evaluation of oxidation characteristic for the trial production of SiC/C compositionally gradient carbon and SiC/C compositionally gradient carbon fiber reinforced carbon (CFRC) materials, which are composed of a surface SiC coating layer, an intermediate SiC/C layer and substrate material, the oxidation test in air at 800°C for up to 100 h was performed compared with each other three kinds version, i.e., substrate material, one with intermediate SiC/C layer and one coated by SiC layer.

It was shown that SiC/C compositionally gradient material exhibited the best oxidation resistance among each substrate series, and the conception of SiC/C compositionally gradient material could be applied to carbon and CFRC materials as well as graphite material.

Keywords: Compositionally Gradient Material, SiC, SiC Coating, Carbon, Carbon Fiber Reinforced Carbon, Oxidation

耐酸化性SiC／C傾斜組成材料の開発

日本原子力研究所東海研究所材料研究部
藤井貴美夫・中野　純一・新藤　雅美

（1994年1月5日受理）

表面SiC被覆層、SiC／C中間層及び基材から構成されるSiC／C傾斜組成炭素材及びSiC／C傾斜組成炭素繊維強化炭素材の試作材の酸化特性を評価するため、各試作材のSiC／C傾斜組成材以外の3種類の材料、すなわち基材、SiC／C中間層付の基材及び表面SiC被覆基材、とともに８００℃の空気中で最長１００時間まで酸化試験を実施した。

炭素材及び炭素繊維強化炭素材系ともにSiC／C傾斜組成材が最も優れた耐酸化性を示すこと及びSiC／C傾斜組材の概念が黒鉛材同様炭素材及び炭素繊維強化炭素材に適応できることを明らかにした。

東海研究所：〒319-11　茨城県那珂郡東海村白方字白根2－4

Contents

目　　次

1. Introduction

The development study of oxidation resistant carbon and graphite materials including carbon fiber reinforced carbon (CFRC) has been performed for wider utilization of these materials in various engineering fields such as nuclear power systems, avitation, spacecraft, etc. As an oxidation resistant material, SiC/C compositionally gradient material is focused. The surface layer of the material hardly peels off compared with normal SiC coated materials because of the gradient in concentration of SiC from the surface to the inside.

As for a graphite material, SiC/C compositionally gradient graphite material has been developed [1-3], and the developed material has exhibited an exellent thermal cyclic characteristic in oxidative environment at high temperatures [3]. The SiC/C compositionally gradient graphite material, which is composed of a surface SiC coating layer, an intermediate SiC/C layer and graphite matrix, is produced by a combination of the reaction between gaseous SiO and graphite, and chemical vapor deposited SiC coating, see fig. 1.

This report describes the results of oxidation test for the trial production of SiC/C compositionally gradient carbon and SiC/C compositionally gradient CFRC materials produced by the same method as the SiC/C compositionally gradient graphite material.

2. Experimental Procedure

2.1 Materials

Materials used as substrate are two kinds of carbon materials, i.e., ASR-1RB and C-140X, and one CFRC, CX-21. From CX-21 which is two direction CFRC, two specimens were prepared by machining in parallel ($\parallel$) and vertical ($\perp$) to fiber direction. Major standard characteristic values [4,5] of those materials are listed up in table 1.

2.2 Production of SiC/C compositionally gradient material

The SiC/C compositionally gradient material is composed of a surface SiC coating layer, an intermediate SiC/C layer and a substrate material.

2.2.1 Formation of intermediate SiC/C layer

Materials used for formation of intermediate SiC/C layer were substrate material and solid SiO of 99.9 % purity. The substrate sample was in the form of a cylinder, 20 mm in length and 10 mm in diameter, with convex sides. The intermediate SiC/C layer was formed by the following reaction in a high purity helium stream at the reaction temperature of 1380 ℃ and the SiO gasification temperature of 1300 ℃,

$$2\ C\ (solid) + SiO\ (gas) \rightarrow SiC\ (solid) + CO\ (gas) \quad \cdots\cdots\cdots\cdots \quad ①$$

After the reaction ①, the mass gain was observed due to the formation of SiC. Larger mass gain means higher SiC content and deeper SiC/C layer in the substrate sample. The specimens with various intermediate SiC/C layers, Si contents of which were 0.38~4.65 %, prepared by controlling the reaction time of ①.

2.2.2 SiC coating by chemical vapor deposition (CVD)

The SiC/C compositionally gradient material is produced by CVD SiC coating on the substrate material with intermediate SiC/C layer. The SiC coating thickness by CVD was around 100 μm.

For comparison, SiC coated substrate materials without intermediate SiC/C layer were prepared by the same coating condition as that for the SiC/C compositionally gradient material for all substrate materials.

The all surface SiC coating by CVD were performed by the outside with considering that the temperature of basic materials was kept lower than 1380 ℃ of the reaction ① because of maintenance of SiC/C compositionally gradient in the intermediate SiC/C layer.

2.3 Oxidation test

The oxidation test was carried out in air at 800 ℃ for up to 100 h. The specimens tested were SiC/C compositionally gradient material with various intermediate SiC/C layers (SiC-SiC/substrate), Si coated substrate (SiC-substrate), substrate with various intermediate SiC/C layers (SiC/substrate) and virgin substrate for four kinds of substrate, i.e., for ASR-1RB series the SiC-SiC/1RB, the SiC-1RB, SiC/1RB and ASR-1RB, for C-140X series the SiC-SiC/140X, SiC-140X, SiC/ 140X and C-140X, for CX-21(∥) series the SiC-SiC/21(∥), the SiC-21(∥), the SiC/21(∥) and CX-21(∥), and for CX-21(⊥) series the SiC-SiC/21(⊥), the SiC-21(⊥), the SiC/21(⊥) and CX-21(⊥).

The oxidation behavior was evaluated by mass measurement.

3. Results and Discussion

The mass loss curves of all tested specimens are summarized in fig. 2. In this figure, all data points were averaged values. The mass loss for carbon and graphite materials is caused by the reaction between carbon and oxygen,

$$2\ \mathrm{C}\ (\text{solid}) + \mathrm{O_2}\ (\text{gas}) \rightarrow 2\ \mathrm{CO}\ (\text{gas}) \cdots\cdots\cdots\cdots\cdots\cdots ②.$$

On the other hand, SiC is oxidized by the following reaction in air,

$$\mathrm{SiC}\ (\text{solid}) + 2\ \mathrm{O_2}\ (\text{gas}) \rightarrow \mathrm{SiO_2}\ (\text{solid}) + \mathrm{CO_2}\ (\text{gas}) \cdots\cdots ③,$$

and the formed very thin SiO_2 layer on SiC is so stable up to around 1000 ℃ [6]. During the surface SiC coating layer maintains its integrity, the specimens coated by SiC layer exhibit no significant mass loss [2,3]. Therefore, the observed mass losses of the specimens coated by SiC layer mean that the surface SiC coating layers have some defects such as cracks, etc.

3.1 Oxidation behavior of substrate series

3.1.1 ASR-1RB

Fig. 3 shows the mass loss curves of the SiC-SiC/1RB, the SiC-1RB, the SiC/1RB and ASR-1RB. This figure indicated that only the intermediate SiC/C layer hardly improved the oxidation resistance of ASR-1RB, however, for surface SiC coating the existence of intermediate SiC/C layer was effective, and the SiC-SiC/1RB exhibited a perfect oxidation resistance.

The order of oxidation resistance was the SiC-SiC/1RB > the SiC-1RB > the SiC/1RB ≧ ASR-1RB.

3.1.2 C-140X

Fig. 4 shows the mass loss curves of the SiC-SiC/140X, the SiC-140X, the SiC/140X and C-140X. The tendency of comparative behavior for four kinds of specimens was similar to that of ASR-1RB series, although the SiC-SiC/140X did not exhibit a perfect oxidation resistance.

The order of oxidation resistance was the SiC-SiC/140X > the SiC-140X > the SiC/140X ≧ C-140X.

3.1.3 CX-21(∥)

Fig. 5 shows the mass loss curves of the SiC-SiC/21(∥), the SiC-21(∥), the SiC/21(∥) and CX-21(∥). The existence of the interemediate SiC/C layer improved the oxidation resistance of CX-21(∥) as well as surface SiC coating, which means that surface SiC coating layer on CX-21(∥) has many defects. The SiC-SiC/21(∥) exhibited the best oxidation resistance, although the oxidation rate was near those of the SiC-21(∥) and the SiC/21(∥).

The order of oxidation resistance was the SiC-SiC/21(∥) > the SiC-21(∥) ≧ the SiC/21(∥) > CX-21(∥).

3.1.4 CX-21(⊥)

Fig. 6 shows the mass loss curves of the SiC-SiC/21(⊥), the SiC-21(⊥), the SiC/21(⊥) and CX-21(⊥). The tendency of comparative behavior for four kinds of specimens was similar to that of CX-21(∥) series, although the oxidation rate of SiC-SiC/21(⊥) was so lower than those of the SiC-21(⊥) and the SiC/21(⊥).

The order of oxidation resistance was the SiC-SiC/21(⊥) > the SiC-21(⊥) ≧ the SiC/21(⊥) > CX-21(⊥).

In conclusion, for each substrate series the SiC-SiC/substrate, i.e., SiC/C compositionally gradient material exhibited the best oxidation resistance.

3.2 Comparison among substrate

The mass loss curves of four virgin substrate materials, i.e., ASR-1RB, C-140X, CX-21(∥) and CX-21(⊥), are shown in fig. 7.

The mass loss curves of four kinds of the substrate with intermediate SiC/C layer, i.e., SiC/1RB, SiC/140X, SiC/21(∥) and SiC/21(⊥), are given in fig. 8. In this figure, all data points were averaged ones among each value of the intermediate SiC/C layers with different Si contents. This figure indicated that the improvement of oxidation resistance of the CFRC by the formation of intermediate SiC/C layer was more effective compared with carbon materials.

The mass loss curves of four kinds of SiC coated substrate, i.e., SiC-1RB, SiC-140X, SiC-21(∥) and SiC-21(⊥), are given in fig. 9, which indicated that contrary to fig. 8 the improvement of oxidation resistance of the CFRC by the surface SiC coating was not so effective compared with carbon materials.

The mass loss curves of four kinds of SiC/C compositionally gradient materials, i.e., SiC-SiC/IRB, SiC-SiC/140X, SiC-SiC/21(∥) and SiC-SiC/21(⊥), are given in fig. 10. The tendency of comparative behavior for four kinds of specimens was similar to that of SiC coated substrate series in fig. 9.

For evaluation of the influence of Si contents in the intermediate SiC/C layers on the oxidation behavior of SiC/C compositionally gradient materials, mass losses of the SiC-SiC/140X after 30 h and of the SiC-SiC/21(∥) after 11 h as a function of Si contents in the intermediate SiC/C layers are plotted in fig. 11. It can be made clear from this figure that the oxidation behavior was independent of the Si contents. It might be caused by the counterbalanced effect between the increases of Si content as an advantage and the increase of porosity as a disadvantage [3].

3.3 Thermal stress

Thermal stress in a two component composite [7] is indicated by

$$\sigma_1=(E_1E_2V_2\Delta\alpha\Delta T)/[(1-\nu)E_1(1-V_2)+E_2V_2] \quad\cdots\cdots\cdots\cdots \quad ④,$$

where σ_1 is thermal stress in component 1, E is Young's modulus, ν is Poisson's ratio, V is volume fraction, $\Delta\alpha$ is thermal expansion coefficient mismatch, ΔT is temperature difference and suffixes 1 and 2 mean two components. If the transverse constraint is negligible,

$$\sigma_1=(E_1E_2V_2\Delta\alpha\Delta T)/[E_1(1-V_2)+E_2V_2] \quad\cdots\cdots\cdots\cdots \quad ⑤.$$

The thermal stress induced in a surface SiC coating layer of a SiC coated material under cooling process was calculated by the equation ⑤, where suffixes 1 and 2 are a SiC coating layer and a substrate material, respectively, V_1/V_2 (sectional area ratio: $[\pi(5.1)^2-\pi(5)^2]/\pi(5)^2$) is 0.04/0.96 and ΔT is

780℃ (800-20℃). Moreover, the thermal expansion coefficient and the Young's modulus of β-SiC are 4.7×10^{-6}/K and 386 GPa [8], respectively.

The caluculated thermal stresses in the surface SiC coating layers of the SiC-1RB, the SiC-140X and the SiC-21(//) are given in table 2. In this table, the positive and negative figures mean tensile and compressive stresses, respectively.

The stability, etc. of a surface SiC coating layer are strongly dependent on thermal stress magnitude. It can be, therefore, expected that the order of the stability of the surface coating layer is equal to the order of the magnitude of the induced thermal stress, i.e., SiC-1RB > SiC-140X > SiC-21(//). This expectation corresponded to the experimental results in fig. 9.

4. Summary and Conclusions

For the evaluation of oxidation characteristic for the trial production of SiC/C compositionally gradient carbon and SiC/C compositionally gradient CFRC materials, which are composed of a surface SiC coating layer, an intermediate SiC/C layer and a substrate material, the oxidation test in air at 800 ℃ for up to 100 h was performed together with each other three kinds version, i.e., substrate material, one with intermediate SiC/C layer and one coated by SiC layer.

The conclusions obtained were as follows;

(1) The SiC/C compositionally gradient material exhibited the best oxidation resistance among each substrate series.

(2) The existence of the intermediate SiC/C layer was effective for surface SiC coating, even though the substrate material was not appropriate one for SiC coating.

(3) The conception of SiC/C compositionally gradient material could be applied to carbon and CFRC materials as well as graphite material.

References

[1] K. Fujii, H. Imai, S. Nomura and M. Shindo, J. Nucl. Mater., 187(1992)204.

[2] K. Fujii, J. Nakano and M. Shindo, J. Nucl. Mater., 203(1993)10.

[3] J. Nakano, K. Fujii and M. Shindo, JAERI-M 93-153(1993).

[4] Steering Committee on VHTR Project, Report of Working Group for Core Support Floor (Private Communication).

[5] CX Series, Catalog of Toyo Tanso Co., Ld.

[6] K. Motzfeldt, Acta Chem. Scand. 18(1964)1596.

[7] H. Takeda and M. Morita, Thermal Stresses in Sapphire/ Nickel Composites, Proc. ICCM-I, p.506 (Boston, 1975).

[8] G. V. Samsonov and I. M. Vinitskij, Data Book for High Melting Point Compounds, translated into Japanese by the Translation Group of Nisso Tsushinsha, Nisso Tsushinsha (1976).

Table 1. Major standard characteristic values of carbon materials (ASR-1RB and C-140X) and CFRC material (CX-21).

Material	Carbon	Carbon	CFRC
Brand	ASR-1RB [4]	C-140X [4]	CX-21 [5]
Bulk density (10^3kg/m^3)	1.74	1.57	1.65
Mean bend strength(MPa)	22.5	6.62	206(∥)
Mean compressive strength (MPa)	93.3	26.1	304(∥) 108(⊥)
Young's modulus (GMa)	14.9	6.8	108(∥)
Mean thermal expansion coefficient (10^{-6}/K)	5.2 (293~673K)	3.5 (293~673K)	0.4(∥) 9(⊥) (RT~1273K)
Thermal conductivity (W/mK) (RT)	11	10.7	49(∥) 7(⊥)

Table 2. Thermal stresses induced in surface SiC coating layers.

Material	Thermal stress (GMa)
SiC-21(∥)	113×10^4
SiC-140X	11×10^4
SiC-1RB	-7×10^4

(1) As -received carbon or graphite material

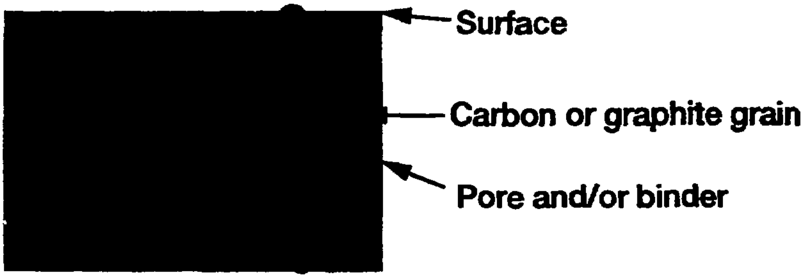

(2) First process ;
Formation of intermediate SiC/C layer by reaction of
$2C(s)+SiO(g)=SiC(s)+CO(g)$

(3) Second process ;
Surface SiC coating by CVD

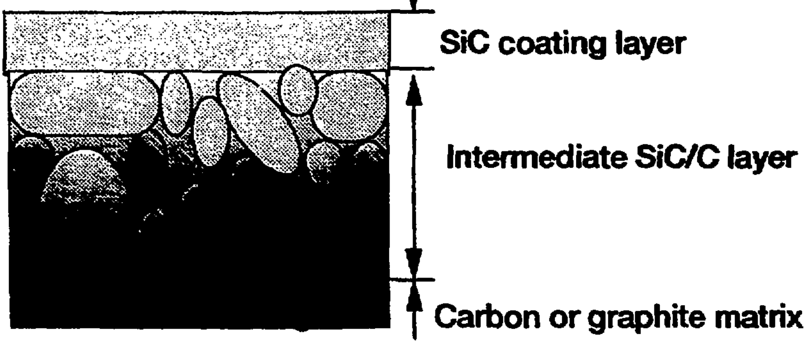

Fig. 1. Production method of SiC/C compositionally gradient material.

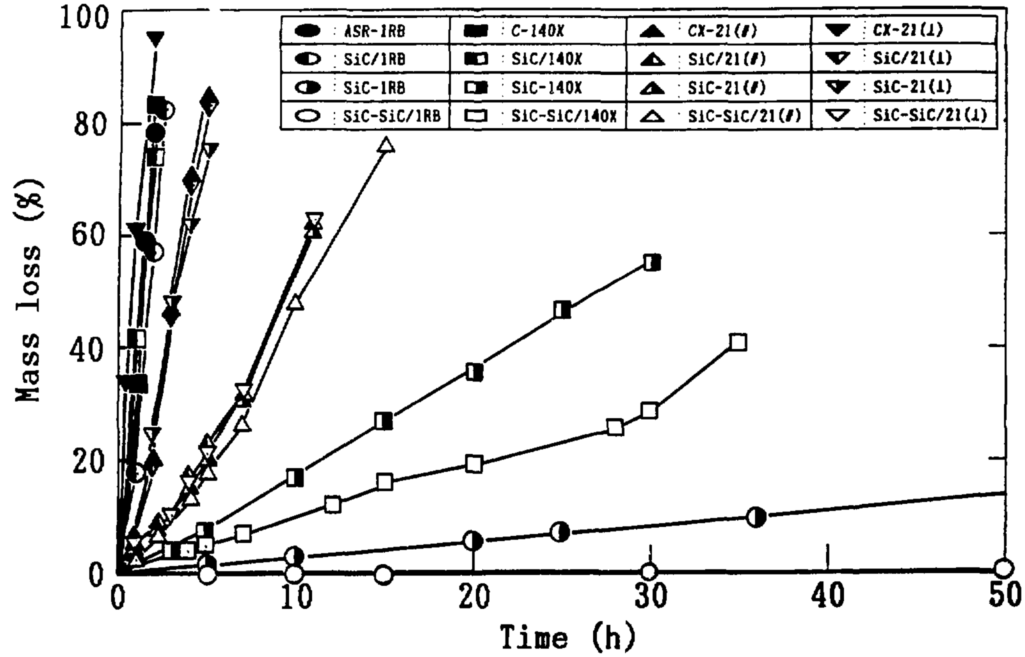

Fig. 2. Mass loss curves of all tested specimens.

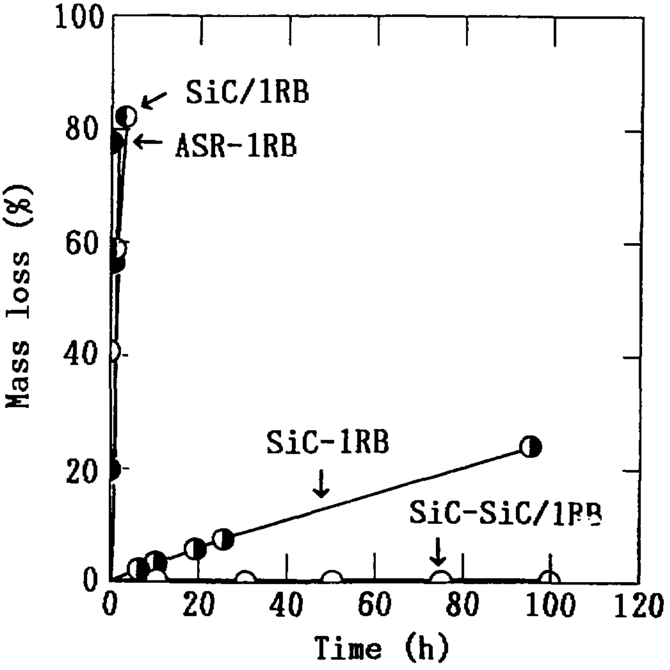

Fig. 3. Mass loss curves of ASR-1RB series.

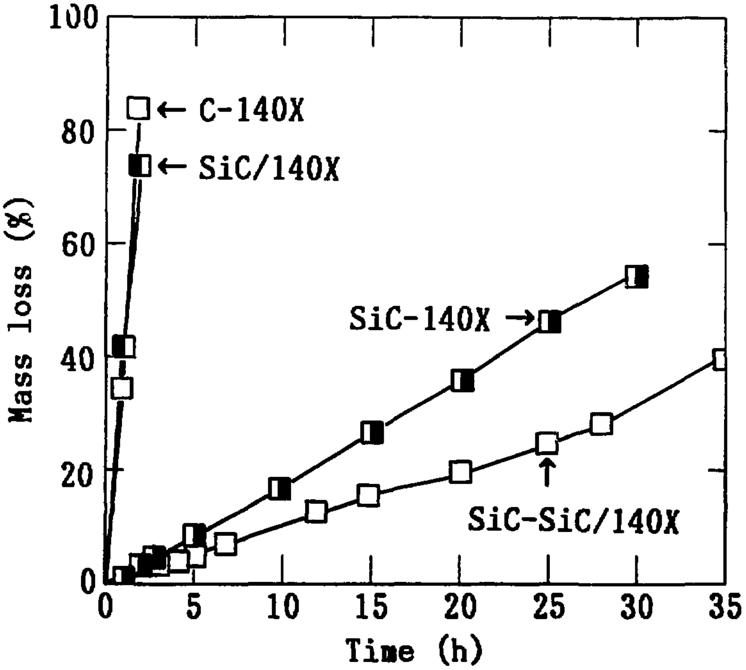

Fig. 4. Mass loss curves of C-140X series.

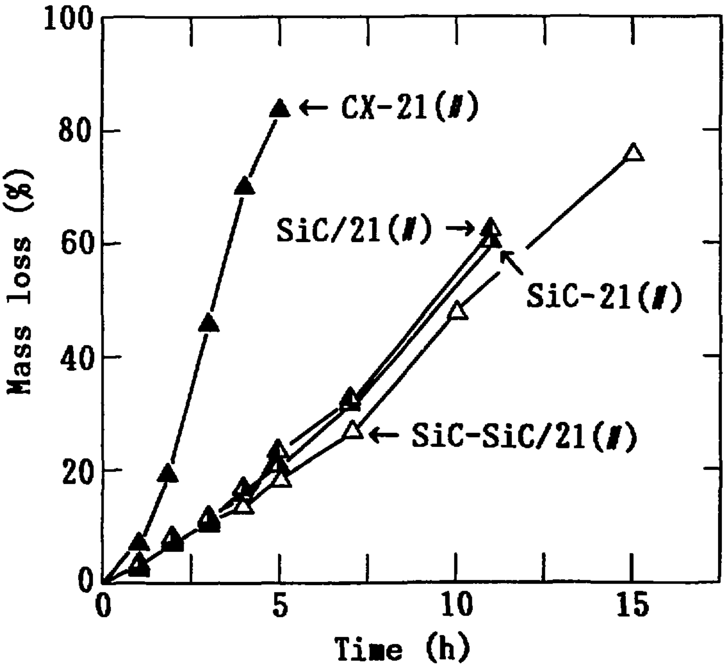

Fig. 5. Mass loss curves of CX-21(//) series.

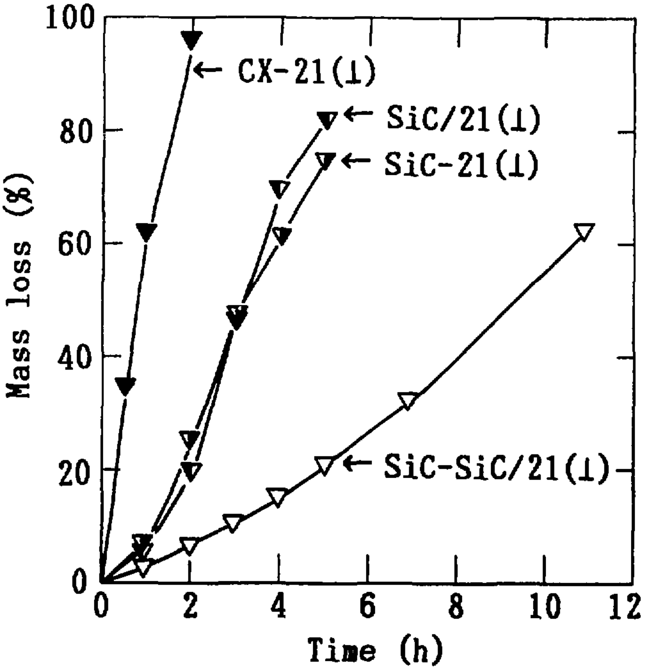

Fig. 6. Mass loss curves of CX-21(⊥) series.

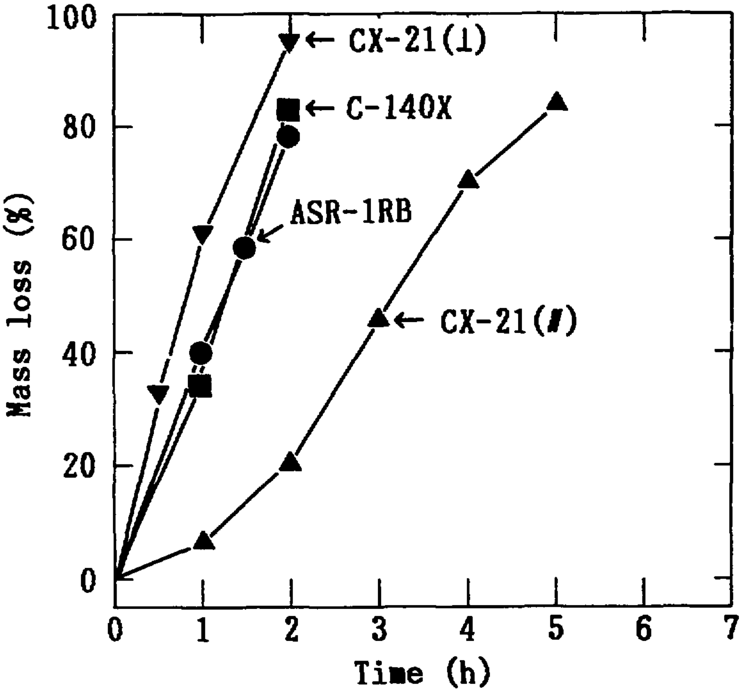

Fig. 7. Mass loss curves of substrate materials.

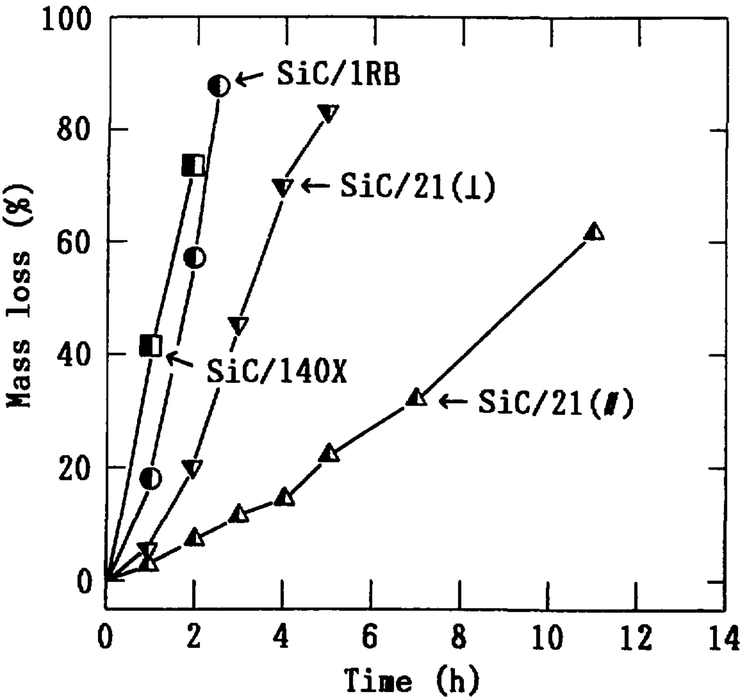

Fig. 8. Mass loss curves of substrate materials with intermediate SiC/C layer.

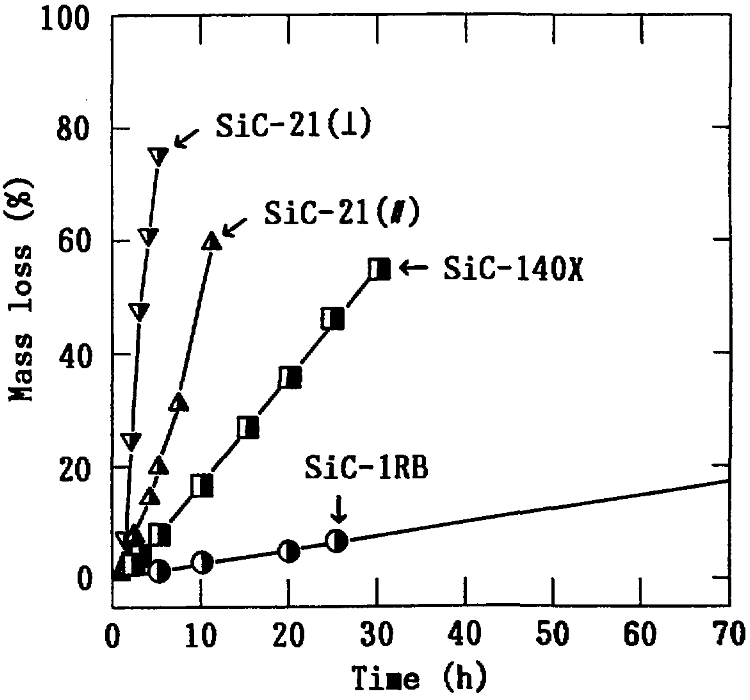

Fig. 9. Mass loss curves of SiC coated substrate materials.

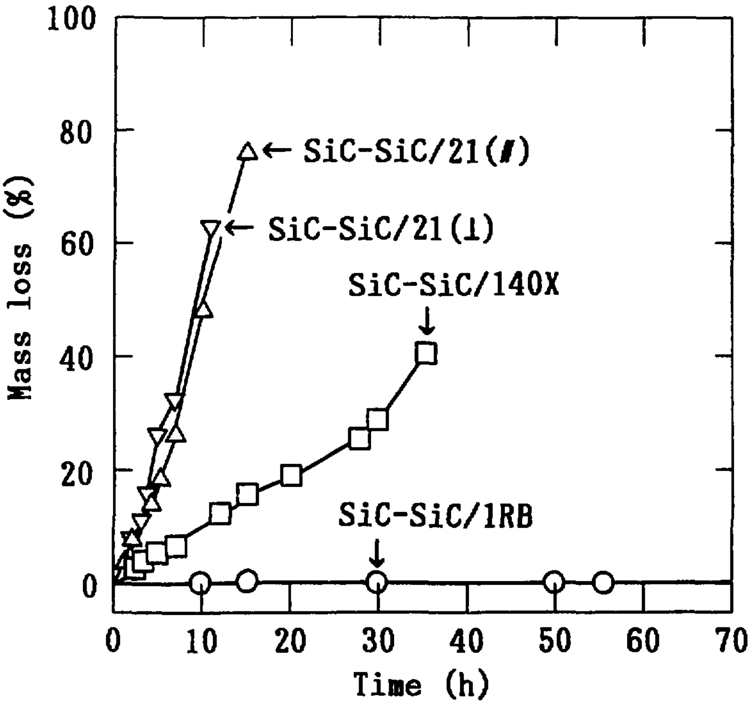

Fig. 10. Mass loss curves of SiC/C compositionally gradient materials.

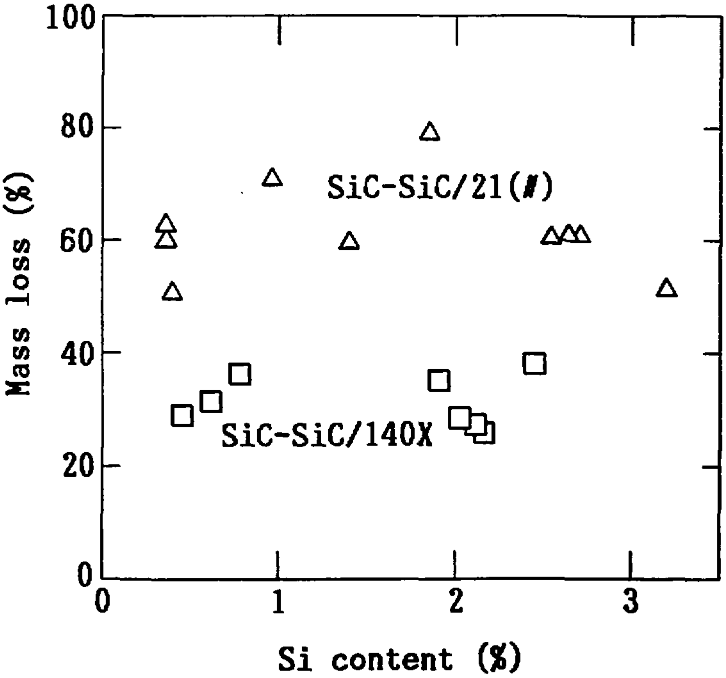

Fig. 11. Mass losses of SiC-SiC/140X after 30 h and of SiC-SiC/21(//) after 11 h as a function of Si contents in intermediate SiC/C layers.

国際単位系 (SI) と換算表

表1　SI基本単位および補助単位

量	名　称	記　号
長　さ	メートル	m
質　量	キログラム	kg
時　間	秒	s
電　流	アンペア	A
熱力学温度	ケルビン	K
物質量	モル	mol
光　度	カンデラ	cd
平面角	ラジアン	rad
立体角	ステラジアン	sr

表3　固有の名称をもつSI組立単位

量	名　称	記号	他のSI単位による表現
周波数	ヘルツ	Hz	s^{-1}
力	ニュートン	N	$m \cdot kg/s^2$
圧力，応力	パスカル	Pa	N/m^2
エネルギー，仕事，熱量	ジュール	J	$N \cdot m$
工率，放射束	ワット	W	J/s
電気量，電荷	クーロン	C	$A \cdot s$
電位，電圧，起電力	ボルト	V	W/A
静電容量	ファラド	F	C/V
電気抵抗	オーム	Ω	V/A
コンダクタンス	ジーメンス	S	A/V
磁束	ウェーバ	Wb	$V \cdot s$
磁束密度	テスラ	T	Wb/m^2
インダクタンス	ヘンリー	H	Wb/A
セルシウス温度	セルシウス度	℃	
光束	ルーメン	lm	$cd \cdot sr$
照度	ルクス	lx	lm/m^2
放射能	ベクレル	Bq	s^{-1}
吸収線量	グレイ	Gy	J/kg
線量当量	シーベルト	Sv	J/kg

表2　SIと併用される単位

名　称	記　号
分，時，日	min, h, d
度，分，秒	°, ′, ″
リットル	l, L
トン	t
電子ボルト	eV
原子質量単位	u

$1\ eV = 1.60218 \times 10^{-19}\ J$

$1\ u = 1.66054 \times 10^{-27}\ kg$

表4　SIと共に暫定的に維持される単位

名　称	記　号
オングストローム	Å
バーン	b
バール	bar
ガル	Gal
キュリー	Ci
レントゲン	R
ラド	rad
レム	rem

$1\ Å = 0.1\ nm = 10^{-10}\ m$

$1\ b = 100\ fm^2 = 10^{-28}\ m^2$

$1\ bar = 0.1\ MPa = 10^5\ Pa$

$1\ Gal = 1\ cm/s^2 = 10^{-2}\ m/s^2$

$1\ Ci = 3.7 \times 10^{10}\ Bq$

$1\ R = 2.58 \times 10^{-4}\ C/kg$

$1\ rad = 1\ cGy = 10^{-2}\ Gy$

$1\ rem = 1\ cSv = 10^{-2}\ Sv$

表5　SI接頭語

倍数	接頭語	記　号
10^{18}	エクサ	E
10^{15}	ペタ	P
10^{12}	テラ	T
10^{9}	ギガ	G
10^{6}	メガ	M
10^{3}	キロ	k
10^{2}	ヘクト	h
10^{1}	デカ	da
10^{-1}	デシ	d
10^{-2}	センチ	c
10^{-3}	ミリ	m
10^{-6}	マイクロ	μ
10^{-9}	ナノ	n
10^{-12}	ピコ	p
10^{-15}	フェムト	f
10^{-18}	アト	a

（注）

1. 表1－5は「国際単位系」第5版，国際度量衡局 1985年刊行による。ただし，1 eV および 1 u の値は CODATA の1986年推奨値によった。
2. 表4には海里，ノット，アール，ヘクタールも含まれているが日常の単位なのでここでは省略した。
3. bar は，JISでは流体の圧力を表わす場合に限り表2のカテゴリーに分類されている。
4. EC閣僚理事会指令では bar，barn および「血圧の単位」mmHg を表2のカテゴリーに入れている。

換　算　表

力	N（$=10^5$ dyn）	kgf	lbf
	1	0.101972	0.224809
	9.80665	1	2.20462
	4.44822	0.453592	1

粘　度　1 Pa·s(N·s/m²) = 10 P（ポアズ）(g/(cm·s))

動粘度　1 m²/s = 10⁴ St（ストークス）(cm²/s)

圧力	MPa（=10 bar）	kgf/cm²	atm	mmHg（Torr）	lbf/in²（psi）
	1	10.1972	9.86923	7.50062×10^3	145.038
	0.0980665	1	0.967841	735.559	14.2233
	0.101325	1.03323	1	760	14.6959
	1.33322×10^{-4}	1.35951×10^{-3}	1.31579×10^{-3}	1	1.93368×10^{-2}
	6.89476×10^{-3}	7.03070×10^{-2}	6.80460×10^{-2}	51.7149	1

エネルギー・仕事・熱量	J（$=10^7$ erg）	kgf·m	kW·h	cal（計量法）	Btu	ft·lbf	eV
	1	0.101972	2.77778×10^{-7}	0.238889	9.47813×10^{-4}	0.737562	6.24150×10^{18}
	9.80665	1	2.72407×10^{-6}	2.34270	9.29487×10^{-3}	7.23301	6.12082×10^{19}
	3.6×10^6	3.67098×10^5	1	8.59999×10^5	3412.13	2.65522×10^6	2.24694×10^{25}
	4.18605	0.426858	1.16279×10^{-6}	1	3.96759×10^{-3}	3.08747	2.61272×10^{19}
	1055.06	107.586	2.93072×10^{-4}	252.042	1	778.172	6.58515×10^{21}
	1.35582	0.138255	3.76616×10^{-7}	0.323890	1.28506×10^{-3}	1	8.46233×10^{18}
	1.60218×10^{-19}	1.63377×10^{-20}	4.45050×10^{-26}	3.82743×10^{-20}	1.51857×10^{-22}	1.18171×10^{-19}	1

1 cal = 4.18605 J（計量法）
= 4.184 J（熱化学）
= 4.1855 J（15 ℃）
= 4.1868 J（国際蒸気表）

仕事率　1 PS（仏馬力）
= 75 kgf·m/s
= 735.499 W

放射能	Bq	Ci
	1	2.70270×10^{-11}
	3.7×10^{10}	1

吸収線量	Gy	rad
	1	100
	0.01	1

照射線量	C/kg	R
	1	3876
	2.58×10^{-4}	1

線量当量	Sv	rem
	1	100
	0.01	1

（86年12月26日現在）